

**FUNCTIONAL ANALYSIS OF THE INHIBITION OF TOPOISOMERASE II
ALPHA BY LINKER HISTONE H1**

A Thesis
Presented to
The Academic Faculty

By

Hiba Hamdan

In Partial Fulfillment
Of the Requirements for the Degree
Master of Science in the
School of Biology

Georgia Institute of Technology

August 2014

Copyright © Hiba Hamdan 2014

**FUNCTIONAL ANALYSIS OF THE INHIBITION OF TOPOISOMERASE II
ALPHA BY LINKER HISTONE H1**

Approved by:

Dr. Yuhong Fan, Advisor
School of Biology
Georgia Institute of Technology

Dr. Francesca Storici
School of Biology
Georgia Institute of Technology

Dr. Adeboyega "Yomi" Oyelere
School of Chemistry and Biochemistry
Georgia Institute of Technology

Date Approved: June 13th, 2014

{وَقُلْ رَبِّ زِدْنِي عِلْمًا} [طه:114]

And say, "My Lord, increase me in knowledge". (The Holy Quran 20:114)

DEDICATION

To my first teacher and biggest inspiration,
in a time when the road for truth is perilous and dim,

To the light, peace be upon Him...

To my esteemed professors who left springs

From which I learned so many things...

To everyone – family and friends – in my present and past
Whether they said a word or whose contributions were vast...

To everyone dead and alive

With whom I learned to strive

To open my mind and try to understand

Life, the priceless gift we have at hand...

With heart-felt prayers for our knowledge to increase

I dedicate this humble piece

ACKNOWLEDGEMENTS

I would like to express my sincere gratitude to my advisor, Dr. Yuhong Fan, for her guidance, continuous encouragement, enthusiasm, patience, and support throughout my graduate research experience at Georgia Tech. I tremendously appreciate all the time she dedicated for the completion of this work and for my personal development as a researcher.

Secondly, I would like to thank my thesis committee members, Dr. Francesca Storici and Dr. Yomi Oyelere, for their valuable suggestions, inputs, and insights despite their busy schedules.

Also, I would like to acknowledge all my lab-mates, past and present, for their constant support and friendship. I am indebted for Samantha Lasater, Yunzhe Zhang, Magdalena Medrzycki, Jin Xu, Zhou Lan, Chen-Yi Pan, ZhiQiang Lin, and especially Kiaxiang Cao and Po-Yi Ho, for troubleshooting problematic experiments, passing on their wisdom and technical expertise, providing hours of explanation, and answering my endless questions. Without their cooperation, openness, patience, and support, this study wouldn't have seen the light!

I would also like to thank the Fulbright program and the U.S. Department of State for providing me with the great venue to grow as a leader, learn from the best, enhance mutual understanding, and become a step closer to reaching my dream.

Last but not least, I would like to thank my dearest mother for her constant prayers and encouragement. I am also grateful to my father, brother, and wonderful family for their enthusiasm, faith, support, and never-ending and unconditional love.

As for all my friends and professors who stood by me all these years, your blessings and encouragement mean the world to me.

Although words are too little to express my feelings and gratitude, thank you all very much! I hope you are all very proud.

TABLE OF CONTENTS

ACKNOWLEDGEMENTS v

LIST OF TABLES viii

LIST OF SYMBOLS AND ABBREVIATIONS x

SUMMARY xii

CHAPTERS:

 CHAPTER 1: Introduction 1

 CHAPTER 2: Materials and Methods 8

 CHAPTER 3: Results 19

 3.1 Analysis of the differential expression patterns of individual linker histone H1 variants in HeLa and HeLa/H1.3(H) cells 19

 3.2 Top2 co-localizes with linker histone H1 in vivo 23

 3.3 Over-expressing hH1.3 in HeLa cells leads to increased cell population with abnormal chromosomes 23

 3.4 Over-expressing hH1.3 in HeLa cells inhibits cell growth 25

 3.5 H1 inhibition of Top2a does not proceed via the Top2a-DNA complex 27

 CHAPTER 4: Discussion and Conclusion 29

REFERENCES 33

LIST OF TABLES

Table 1. List of Primary and Secondary Antibodies	11
Table 2. Acetonitrile gradient for HPLC analysis.....	14
Table 3. Primer list for qRT-PCR analysis of FLAG-H1s and GAPDH	18

LIST OF FIGURES

Figure 1. Topoisomerase II alpha relieves topological stress in DNA.	2
Figure 2. Structure and function of linker histone H1.	4
Figure 3. Analysis of total histone extracts from HeLa and HeLa/H1.3(H) cells.....	20
Figure 4. Western blotting analysis of total histone extracts from HeLa and HeLa/H1.3(H) cells.....	21
Figure 5. qRT-PCR analysis of mRNA levels of FLAG-tagged linker histone subtypes in HeLa and HeLa/H1.3(H) cells.	21
Figure 6. Overexpression of linker histone H1.3 increases total H1 levels and changes H1 composition in HeLa cells.....	22
Figure 7. Top2a co-localizes with H1 <i>in vivo</i>	23
Figure 8. Over-expressing hH1.3 in HeLa cells leads to increased cell population with abnormal chromosomes.	25
Figure 9. Over-expressing hH1.3 in HeLa cells leads to delayed growth and decreased metabolic activity.....	26
Figure 10. H1 inhibition of Top2a does not proceed via the Top2-DNA complex.	28
Figure 11. Working Model of the interaction of H1 and Top2a and the effect of the inhibition on chromosome condensation and segregation	30

LIST OF SYMBOLS AND ABBREVIATIONS

aa: amino acid

cDNA: complementary DNA

CTD: C-terminal domain

ddH₂O: Deionized Distilled Water

DNA: deoxyribonucleic acid

EMEM α : Eagle's Minimum Essential Medium (also known as Minimum Essential Medium Alpha Medium)

ESC: Embryonic Stem Cell

FBS: Fetal bovine serum

G418: Geneticin

GAPDH: Glyceraldehyde 3-phosphate dehydrogenase

GD: Globular domain

H1: Linker Histone H1

hH1.3: Human histone H1.3 Variant

HPLC: High Performance Liquid Chromatography

mRNA: messenger ribonucleic acid

NTD: N-terminal domain

OD: Optical Density

PBS: Phosphate Buffered Saline

PBS-T: 0.1% Tween-20 in 1xPBS

PCR: polymerase chain reaction

PI: cOmplete Protease Inhibitor

qRT-PCR: quantitative reverse transcriptase polymerase chain reaction

RNA: ribonucleic acid

RP-HPLC: reverse phase high performance liquid chromatography

RPM: revolutions per minute

RT-PCR: reverse-transcription polymerase chain reaction

SDS-PAGE: sodium dodecyl sulfate polyacrylamide gel electrophoresis

TFA: Trifluoroacetic acid

Top2: Topoisomerase II

Top2a: Topoisomerase II α

Topo: Topoisomerase

SUMMARY

In higher eukaryotes, DNA is progressively packaged into chromatin. In these varying levels of compaction, linker histone H1 is a key player for mediating chromatin folding. As a result, linker histone H1 is involved in regulating cellular activities, such as gene transcription. Also essential for multiple cellular processes, topoisomerase II alpha (Top2a) is an enzyme that regulates DNA topology and thus is a target in cancer therapeutics. Previous studies in our lab have identified Top2a as an H1.3 binding partner by immunoprecipitation in embryonic stem cells. Further studies have shown that mouse histone H1.3 inhibits Top2a enzymatic activity *in vitro*. In this thesis, I pursued a functional analysis to confirm and analyze the inhibitory effect of human H1.3 on Top2a *in vivo*. We found that overexpression of hH1.3 significantly suppressed the growth of HeLa cancer cells and resulted in an increased cell population with abnormal mitotic chromosomes. These analyses may lead to a better understanding of the role of H1 and Top2a in chromatin structure and function.

CHAPTER 1

INTRODUCTION

Topoisomerases: An Overview

Topological tension in DNA occurs in a variety of cellular processes, such as transcription, DNA replication, and chromosome segregation (Espeli & Marians, 2004; Larsen, Skladanowski, & Bojanowski, 1996; Luo, Yuan, Chen, & Lou, 2009; McClendon & Osheroff, 2007; Mondal et al., 2003; Wang, 2002). Such topological tension, when left unresolved, leads to DNA breaks and disruption of many cellular processes (McClendon & Osheroff, 2007; Wang, 2002). Topoisomerases, a group of enzymes commonly present in the 'chromosome scaffold', relax topological DNA tensions and resolve chromatin entanglement. Topoisomerases are classified as either type I or type II depending on their mechanisms in altering supercoil topology. Type I topoisomerases transiently cut a single DNA backbone, allowing for the rotation of the resulting sing-stranded DNA around the break. This process is ATP-independent. In comparison, type II topoisomerases, Top2a and Top2b, follow an ATP-dependent procedure involving binding to the DNA-double strand, cutting both strands transiently, pushing the second double-stranded DNA segment through the break, and finally religating both segments (McClendon & Osheroff, 2007; Wang, 2002).

Coordinated action of type I and type II topoisomerases relieves topological perturbations arising from DNA replication and gene transcription (Mondal & Parvin, 2001; Wang, 2002). As the replication machinery advances along the double-stranded DNA, negative and positive supercoils form at the back and front of the machinery

(Figure 1). Top2a resolves the tangled duplex molecules and alleviates the supercoils (Figure 1). Also, Top2a enzymes are key players in resolving supercoils resulting from transcription (McClendon, Rodriguez, & Osheroff, 2005; Mondal & Parvin, 2001).

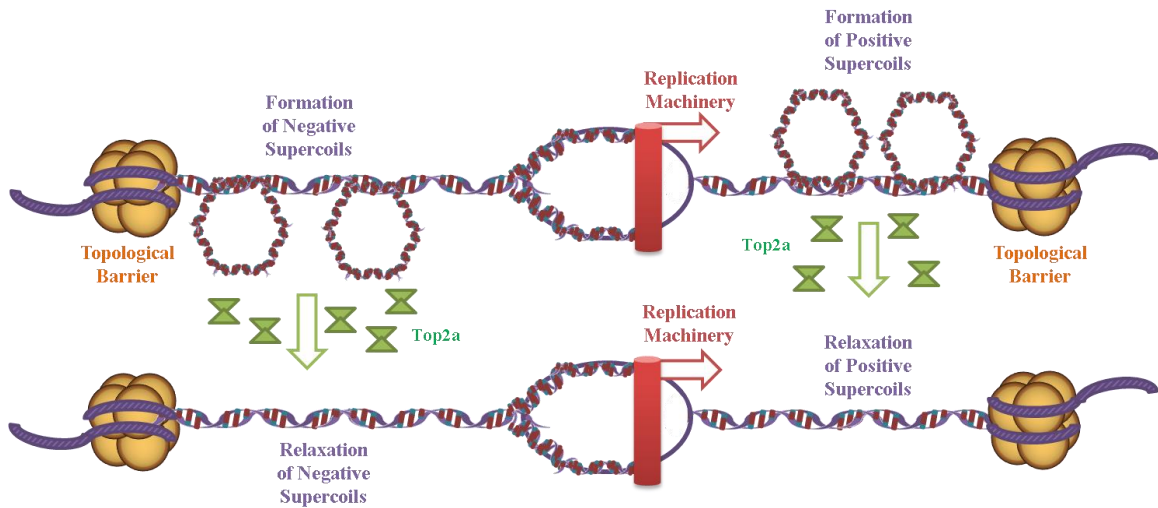


Figure 1. Topoisomerase II alpha relieves topological stress in DNA. As the replication machinery moves along the DNA, negative (under-winding) and positive (over-winding) supercoils form towards the back and front of the replication fork, creating topological DNA stress. Top2a is required to relax the tension and untangle the over-lapping double-stranded DNA segments. A similar process occurs during transcription as the RNA machinery moves along the DNA.

Top2a, identified as a major component of the mitotic chromosome scaffold (Earnshaw, Halligan, Cooke, Heck, & Liu, 1985), is indispensable for cell proliferation. The expression of Top2a is increased in S phase, and peaks during M phase of the cell cycle (Heck, Hittelman, & Earnshaw, 1988; Woessner, Mattern, Mirabelli, Johnson, & Drake, 1991). Top2a is over-expressed in numerous cancer cell lines and tumors (Al-Kuraya et al., 2007; Schrader et al., 2004; Willman & Holden, 2000; Zhao, Yu, Liu, Wang, & Cai, 2008). Therefore Top2a has been a clinical target in cancer therapeutics

and several groups of drugs have been developed. Classes include DNA synthesis inhibitors or fluoroquinolones, DNA replication intercalators or anthracyclins such as doxorubicin, and others (Wong, Oliver, & Linington, 2012). Inhibitors of mammalian topoisomerases, such as camptothecins, etoposide, tenoposide, doxorubicin, are also cytostatic drugs for cancer treatment (Pommier, Leo, Zhang, & Marchand, 2010). Inhibition of topoisomerase II activity by drugs such as etoposide and doxorubicin causes cell cycle arrest in late S and G2 phase (Garrett & Collins, 2011).

Linker Histone H1: In a Nutshell

In eukaryotes, 147 base pairs of DNA are wrapped around the octameric core histone molecules, including two copies of H2A, H2B, H3, and H4, to form the nucleosome (Brown, 2003; Happel & Doenecke, 2009; Horn & Peterson, 2002; Luger, Mader, Richmond, Sargent, & Richmond, 1997; Zlatanova, Bishop, Victor, Jackson, & van Holde, 2009). Linker histone H1 binds to nucleosome at the entry and exit sites of DNA as well as the linker DNA, facilitating the folding of higher order chromatin structure (Figure 2) (Happel & Doenecke, 2009; Wolffe, Khochbin, & Dimitrov, 1997). This binding of H1 also stabilizes the 30 nm fiber (Bednar et al., 1998; Robinson & Rhodes, 2006; Sumner, 2003; Woodcock, Skoultchi, & Fan, 2006), which can be further compacted into 100 and 400 nm interphase fibers.

Linker histone H1 is a family of lysine-rich proteins that has a canonical three domain structure. The tripartite structure includes a highly conserved globular domain (GD: ~75-80 aa), an unstructured long positively charged C-terminal domain (CTD: ~100

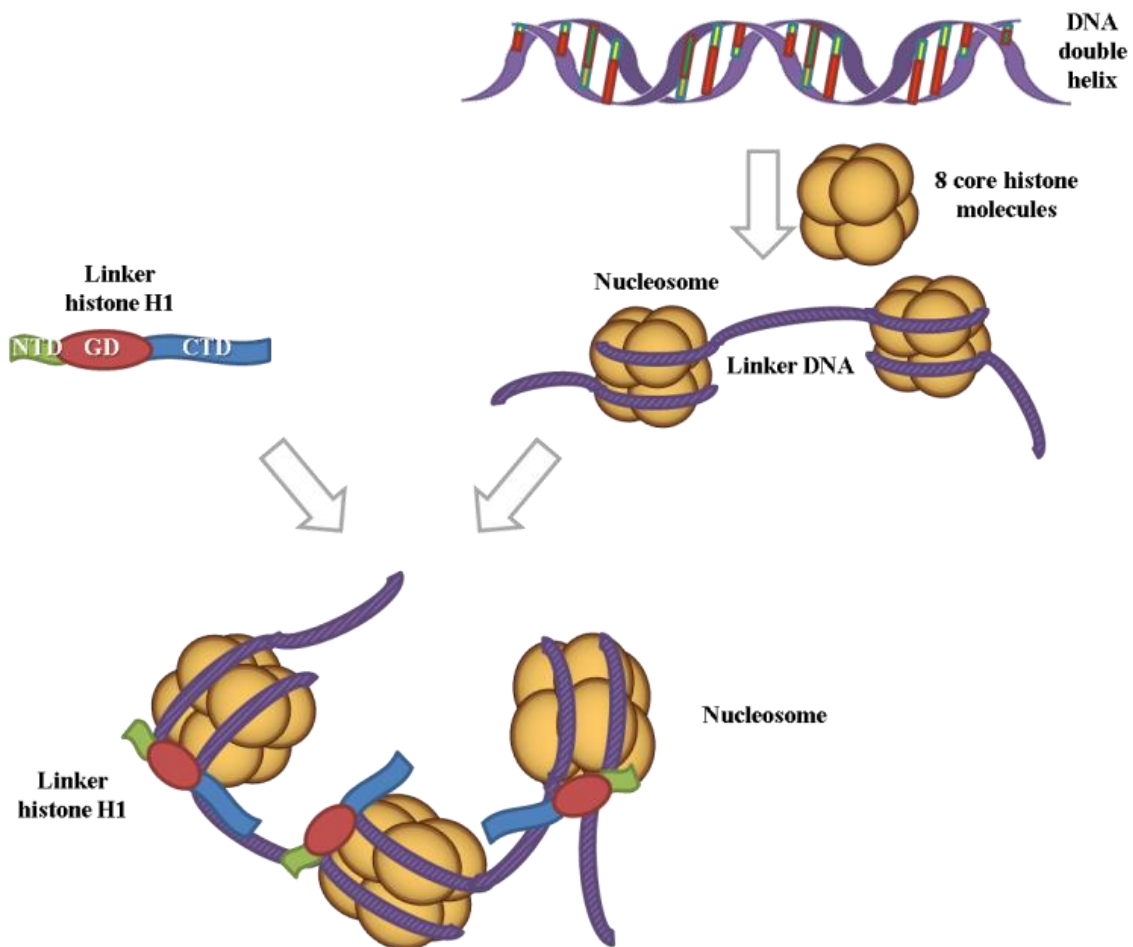


Figure 2. Structure and function of linker histone H1. Linker histone H1 is composed of a tripartite structure with an N-terminal domain (NTD), a globular domain (GD), and a C-terminal domain (CTD). The first level of chromatin condensation involves the wrapping of the double stranded DNA around an octamer of core histone molecules (H2A, H2B, H3, and H4) to form the nucleosome. H1 binds to the nucleosomal DNA and the linker DNA.

aa), and a short basic N-terminal domain (NTD: ~13-45 aa) (Happel & Doenecke, 2009).

The CTD is intrinsically disordered, and its chromatin condensing function and interaction with linker DNA depends on its amino acid sequence (Caterino, Fang, &

Hayes, 2011; Hansen, Lu, Ross, & Woody, 2006; Lu, Hamkalo, Parseghian, & Hansen, 2009). GD contains winged-helix motifs and DNA binding sites, and interacts with the nucleosome (Ramakrishnan, Finch, Graziano, Lee, & Sweet, 1993; Thomas, 1999). Both the GD and the CTDs also function in protein-protein interaction (Montes de Oca, Lee, & Wilson, 2005; Widlak et al., 2005). However, the roles of the NTD in DNA-binding remain unknown (Harshman, Young, Parthun, & Freitas, 2013; McBryant, Lu, & Hansen, 2010).

11 different H1 variants have been identified in mammals, making it the most divergent class of histones (Happel & Doenecke, 2009). In humans, there are one oocyte-specific variant (H1oo), three testes-specific subtypes (H1t, H1T2 and H1LS1), and seven somatic isoforms (H1.1-H1.5, H1.0, and H1x) (Albig, Kardalidou, Drabent, Zimmer, & Doenecke, 1991; Albig, Meergans, & Doenecke, 1997; Happel & Doenecke, 2009; Medrzycki, 2013; Meergans, Albig, & Doenecke, 1997; Th'ng, Sung, Ye, & Hendzel, 2005). The different subtypes have distinctive nucleosomal binding affinities (Misteli, Gunjan, Hock, Bustin, & Brown, 2000), so may differentially modulate chromatin compaction (Brown, 2001; Oberg, Izzo, Schneider, Wrangé, & Belikov, 2012; Th'ng et al., 2005). In addition, expression of the different subtypes is not the same. Among the somatic H1s, the expression of H1.0 and H1x is replication-independent, whereas the expression of H1.1 through H1.5 is dependent on replication (Albig et al., 1997). The levels of H1 subtypes differ in dividing and non-dividing cells. While H1.0 accumulates in cells that are terminally differentiated, the other somatic H1s are ubiquitously expressed with varying levels (Happel & Doenecke, 2009).

Regulatory functions of linker histones include inhibiting the action of chromatin-assembly complexes, modulating the access of regulatory factors and chromatin-specific proteins to their chromatin targets, and restricting the mobility of the nucleosome (Harshman et al., 2013; McBryant et al., 2010; Millan-Arino et al., 2014). In addition to its role in stabilization and condensation of chromatin, H1 functions in specific regulation (repression and activation) of gene expression (Fan et al., 2005; Happel & Doenecke, 2009; Woodcock et al., 2006). H1 depletion in mouse embryonic stem cells alters the global chromatin structure but regulates specific gene expression (Fan et al., 2005). H1 also influences developmental processes in *C. elegans* (Jedrusik & Schulze, 2001). In mice, depletion of individual linker histone H1 variants does not hinder development and show no obvious phenotype, due to the compensatory up-regulation of other subtypes (Fan, Sirotkin, Russell, Ayala, & Skoultchi, 2001; Sirotkin et al., 1995). However, triple H1 (H1c, H1d, and H1e) knockout studies prove H1 to be indispensable for mammalian development (Fan et al., 2003).

Individual H1 variants may function through protein-protein interactions (McBryant et al., 2010). For example, the replacement variant, H1.0, is likely a vital player in the nucleolus, as it is reported to interact with extensive protein networks in nucleolus, involving RNA metabolism, pre-mRNA splicing, rRNA biogenesis, translation, and cellular transport (Kalashnikova et al., 2013). H1.1 has been shown to interact with Barrier-to-autointegration factor (BAF), which may provide access to chromatin (Montes de Oca et al., 2005). H1.2 has been found to repress p53 target genes by forming complexes with p53, the tumor suppressor (K. Kim et al., 2012), and H1.4 was found to recruit heterochromatin protein 1 (HP1) and Polycomb complexes which

lead to gene silencing (Daujat, Zeissler, Waldmann, Happel, & Schneider, 2005). H1 is also involved in apoptosis by interaction with DNA fragment factor 40/Caspase activated DNase (DFF40/CAD) (Liu, Zou, Widlak, Garrard, & Wang, 1999; Widlak et al., 2005).

Previous studies in our lab have identified Top2a as a novel H1.3 binding partner by co-immunoprecipitation in FLAG-H1d-containing embryonic stem cells (Lasater, 2012). Further studies have shown that mouse histone H1 inhibits Top2a activity *in vitro* and that overexpression of its human homolog (hH1.3) in human cancer cells leads to increased cell proportion with defects in chromosome segregation *in vivo* (Lasater, 2012).

In this thesis, we analyzed H1 profiles in a human cervix adenoma cancer cell line, HeLa cells, and investigated the effects of H1.3 overexpression on cell growth and mitotic chromosomes in these cells. Our results suggest a regulatory role of H1 in chromosome function through inhibition of Top2a. These results might lead to a new therapeutic intervention approach of targeting Top2a.

CHAPTER 2

MATERIALS AND METHODS

Cell Culture

HeLa cells (human cervical cancer-derived cell-line) were cultured at 37°C and 5% CO₂ in Minimum Essential Medium Alpha Medium (Gibco, Grand Island, New York) supplemented with 10% Fetal Bovine Serum (FBS; Thermo-Scientific, Waltham, Massachusetts) and 1% penicillin-streptomycin (Corning, Manassas, Virginia). Cell media were changed every 2 days and cells were passaged when they reach about 80% confluency. HeLa/hH1.3 and HeLa/EV stable cell lines, established by transfecting HeLa cells with FLAG-hH1.3 expression vector and empty vector respectively, were cultured with medium supplemented with G418 (1 mg/ml). Transfection of HeLa cells were performed using Lipofectamine 2000 (Invitrogen, Carlsbad, California) according to the manufacturer's recommendations. HeLa/hH1.3 cell lines were established by previous lab graduate Samantha Lasater (Lasater, 2012).

Growth Curve and MTT Assay

The growth curve and MTT assays were performed in parallel to measure cell growth and metabolic activity, respectively. For the growth curve assay, 30,000 cells were seeded per well on a 12-well plate (Corning) in triplicates, with each cell line cultured in 24 wells total. Cells were trypsinized and counted every two days for 12 days.

For the MTT assay, exponentially growing cells were seeded in triplicates at a density of 1,500 cells in 0.1 ml medium per well on a 96-well plate. For each

measurement, 11 μ l of 5mg/ml MTT (3-(4,5-dimethylthiazol-2-yl)-2,5-diphenyltetrazolium bromide) was added to the wells to be analyzed and the plate is incubated at 37°C for 2 hours to allow the reduction of the yellow tetrazole and formation of purple formazan crystals. Then, 111 μ l stop solution (for 50 ml: 25 ml 20% SDS; 50 μ l 37% HCl; ddH₂O) was added and the plate was incubated overnight at 37°C. The absorbance is then read at 570 nm with a micro-plate reader. The acellular wells were included as blank negative controls in the template. The average absorbance were calculated, and plotted to determine the metabolic activity.

Nuclei Purification

When ready to harvest, HeLa cells grown in 15 cm plates (Corning, Manassas, Virginia) were washed with 1xPBS (0.001 M phosphate buffer; 138 mM NaCl; 3 mM KCl; pH 7.4), harvested, and pelleted by centrifugation at 1,500 rpm for 10 minutes at 4°C. The pellet was resuspended in 1xPBS and centrifuged again at 1,500 rpm for 3 minutes. The pellet was subsequently resuspended in RSB Buffer (10 mM NaCl; 3 mM MgCl₂; 10 mM Tris pH 7.5) at 10⁷ cells/ml, and dounced on ice for 20 minutes with an equal volume of RSB buffer containing 0.5% NP-40, 0.5 mM PMSF, and 10 μ l cOmplete Protease Inhibitor (PI) (Roche, Indianapolis, IN) per 10⁷ cells, counted, and centrifuged at 1,100 rpm for 7 minutes at 4°C. Next, pellets were resuspended in 500 μ l RSB/10⁸ cells with 0.5 mM PMSF and PI. The nuclei can be used for nuclear extract preparation or stored at -80°C in 1:1 glycerol to storage buffer (50 mM Tris pH 8.3; 40% glycerol; 5 mM MgCl₂; 0.1 mM EDTA).

Nuclei Extract Preparation

Purified HeLa nuclei were centrifuged at 1,800 rpm for 5 minutes at 4°C. After removing the storage buffer, the pellet of nuclei was resuspended with 400 μ l/ 10^8 cells of buffer C (20 mM HEPES pH 7.9; 0.42 M NaCl; 5 mM MgCl₂; 0.1 mM EDTA; 20% glycerol; 1% Triton-X-100; 1 mM DTT; 0.2 mM PMSF; PI). The tubes were rotated at 4°C for 20 minutes and checked every 5 minutes to prevent clumping, centrifuged at 1,200 g for 5 minutes at 4°C. The supernatant was transferred into dialysis cassettes (Thermo Scientific, Rockford, IL), dialyzed for 2 hours at 4°C in buffer D (20 mM HEPES pH 8.0; 20% (V/V) glycerol; 100 mM KCl; 0.2 mM EDTA; 1 mM DTT; 0.5 mM PMSF), subsequently transferred into new tubes, and stored at -80°C.

Western Blotting

Total protein concentration of each sample was measured using the Bradford Protein Assay (BioRad Life Sciences, Hercules, California). Samples were then denatured in 4x SDS loading dye (200 mM Tris-Cl (pH 7.0); 400 mM DTT; 8% SDS; 20% glycerol) and incubated at 95°C for 3-5 minutes before loading on 10% SDS-Polyacrylamide gels. Proteins were separated at 100 volts for 1.5 hours and transferred to a 0.45 μ m nitrocellulose membrane (BioRad Life Sciences, Hercules, California). Membranes were blocked with 1:1 ratio of Odyssey blocking buffer (Li-Cor Inc., Lincoln, Nebraska) and 1xPBS for 1 hour at room temperature followed by incubation overnight with primary antibodies (table 1) at 4°C with gentle shaking. The membranes were subsequently washed with 0.1% Tween-20 in 1xPBS (PBS-T) and incubated with

secondary antibodies for 1 hour (table 1). Blots were washed with PBS-T and visualized using Odyssey Infrared Imaging System (Li-Cor Inc., Lincoln, Nebraska).

Table 1. List of Primary and Secondary Antibodies

Primary Antibody	Species	Company	Dilution
Anti-Top2a	Rabbit	TopoGEN, Port Orange, Florida	1:10,000
Anti-FLAG	Mouse	Sigma-Aldrich, Saint Louis, Missouri	1:1,000
Anti-H1.0	Rabbit	abcam, Cambridge, Massachusetts	1:1,000
Anti-H1.1	Rabbit	abcam, Cambridge, Massachusetts	1:1,000
Anti-H1.2	Rabbit	abcam, Cambridge, Massachusetts	1:1,000
Anti-H1.3	Rabbit	abcam, Cambridge, Massachusetts	1:1,000
Anti-H1.4	Rabbit	abcam, Cambridge, Massachusetts	1:1,000
Anti-H1.5	Rabbit	abcam, Cambridge, Massachusetts	1:1,000
Secondary Antibody	Species	Company	Dilution
Donkey anti-Mouse	-	Jackson ImmunoResearch, West Grove, Pennsylvania	1:10,000
Goat anti-Mouse	-	Life Technologies, Carlsbad, California	1:10,000
Goat anti-Rabbit	-	Life Technologies, Carlsbad, California	1:10,000

Top2a In-Vivo Link Assay

HeLa/H1.3(H) cells growing in exponential phase were probed for Top2a inhibition using the Topoisomerase II *In Vitro* Link Kit (TopoGEN, Port Orange, Florida). According to the manufacturer's manual, cells were treated with 100 μ M

etoposide. After incubation for 30 minutes at 37°C in 1 ml serum-free medium, cells were counted then lysed by 1% sarkosyl. The lysate was carefully layered on top of a cesium chloride (CsCl) gradient. The polyallomer tubes were then centrifuged at 31,000 RPM for 12 hours at room temperature. Fractions of 0.4 ml each were collected and diluted for OD measurement and identification of Top2-DNA cleavage complexes at 260 nm. The different CsCl fractions were loaded on a nitrocellulose membrane and subjected to vacuum in a slot blot device. Membrane was then incubated with blocking buffer in PBS-T for 2 hours. After western blotting using Top2a antibody, signals were detected using the Odyssey Imaging System (LiCor Biosciences).

Histone Extraction and Purification

Histone extraction and purification were performed as previously described (Medrzycki, Zhang, Cao, & Fan, 2012). Briefly, HeLa cultured in 15 cm plates were harvested and resuspended in 3 ml sucrose buffer (0.3 M sucrose; 15 mM NaCl; 2 mM EDTA; 10 mM HEPES pH 7.9; 0.5 mM PMSF; PI) with 0.5% NP-40, and dounced on ice with a B pestle (Dounce homogenizer) for 10 minutes. Next, the homogenate was centrifuged at 1,575 g for 10 minutes at 4°C after which the pellet is resuspended in 1 ml high salt buffer (0.35 M KCl; 10 mM Tris pH 7.2; 5 mM MgCl₂; 0.5 mM PMSF; PI) and dounced on ice. The homogenates were transferred into eppendorf tubes, incubated on ice for 20 minutes, and centrifuged for 10 minutes at 14,000 rpm, 4°C. The pellet was resuspended in 0.4 ml 0.2N H₂SO₄ (1N=0.5M) using an eppendorf tube pestle dounce and incubated on rotator at 4°C overnight. The following day, the tubes were centrifuged at 14,000 rpm for 10 minutes at 4°C, and the supernatant was transferred into a new tube. Since ample amount of protein was present, 2.5 V of ice cold 100% ethanol was added

directly to the tube, mixed and stored overnight at -20°C. The tubes were centrifuged at 14,000 rpm for 10 minutes at 4°C, and the histone pellet was washed 3 times with 70% ethanol, and air-dried. The resulting pellet was stored at -80°C or used for HPLC analysis.

HPLC analysis of Histones

HPLC analysis of linker histone H1 subtypes was performed as previously described (Fan & Skoultchi, 2004; Medrzycki et al., 2012). Briefly, histone extracts from HeLa and HeLa/H1.3(H) were resuspended in 100µl ddH₂O and injected into a Vydac 218TP C18 reverse-phase column (Grace Davison Discovery Sciences, Deerfield, Illinois) of the GE AKTA Purifier HPLC system (GE Healthcare Life Sciences, Pittsburgh, Pennsylvania). Linker and core histones were fractionated with an increasing acetonitrile gradient with 0.1% Trifluoroacetic acid (TFA) over time as shown in table 2. The effluent was monitored at 214 nm, and histone peaks were collected according to the histone profiles (table 2 & Figure 3). UNICRON 5.11 Software (GE Healthcare Sciences, Pittsburgh, Pennsylvania) was used to record and analyze the HPLC profiles. All protein fractions collected were lyophilized and resuspended in ddH₂O for further analysis. The HPLC peaks were collected and analyzed on a Qstar XL MS/MS system (Applied Biosystems) with ESI (Electrospray ionization). The Mass Spectrometry data were analyzed by Mass Spectrometry Analyst QS software (Applied Biosystems). Identification of histone subtypes attributed to the relative peaks was also confirmed using Western blot. The relative proportions of H1 subtypes as well as the ratio of H1 subtypes to nucleosome core particles were calculated from the normalized A₂₁₄ values of the peaks for the H1 subtypes and H2B of HPLC analysis. A₂₁₄ values were

normalized by the number of peptide bonds of the respective histone proteins. The ratios of the percentage of total H1 and the total H1 per nucleosome ratios were calculated as follows.

$$\text{Percentage of Total H1} = \frac{\text{normalized } A_{214} \text{ of indicated H1 peak}}{\text{normalized Total } A_{214} \text{ of all H1 peaks}}$$

$$\text{Total H1 per nucleosome} = \frac{1}{2} \frac{\text{normalized Total } A_{214} \text{ of all H1 peaks}}{\text{normalized } A_{214} \text{ of H2B}}$$

Table 2. Acetonitrile gradient for HPLC analysis

Time (Minutes)	Acetonitrile / 0.1% TFA (%)	0.1% TFA / ddH₂O (%)
0	0	100
1	5	95
11	25	75
26	30	70
45	35	65
66	40	60
75	43	57
126	55	45
131	90	10
136	5	95

Immunocytochemistry

HeLa cells were grown on glass cover slips in required media (EMEM α) till confluency. Cells were fixed with 4% paraformaldehyde in PBS for 20 minutes followed by permeabilization with 0.2% Triton X-100 in PBS for 30 minutes at room temperature. After washing with 1xPBS, cells were incubated with 10% FBS in PBS overnight. For immunocytochemistry, individual cover slips were incubated with primary antibodies

(Top2a, 1:10,000; M2-FLAG, 1:400) diluted in 10% FBS in PBS for 1 hour in the dark. The coverslips were washed with 0.2% Tween-20 in PBS then incubated with fluorescently labeled secondary antibodies (Goat anti-rabbit, 1:200; Donkey anti-mouse, 1:500) diluted in 10% FBS in PBS for 1 hour in the dark. Nuclei were counter stained with Hoechst dye (1:1,000). After washing with 0.2% Tween-20 in PBS, cells were mounted on a slide using Fluormount G and images were collected on an Olympus Fluorescence Microscope (Olympus America Inc., Center Valley, Pennsylvania) and processed by Q Capture Pro software version 5.1 (Q imaging, Surrey, British Columbia, Canada).

Metaphase Spread

HeLa cells growing in log phase were treated with colcemid (Life Technologies, Carlsbad, California) at 37°C for 60 minutes when 85% confluence, trypsinized, harvested, centrifuged at 900 rpm for 4 minutes at room temperature, resuspended in 1xPBS and centrifuged again at 900 rpm for 4 minutes at room temperature. Cells were subsequently resuspended with pre-warmed hypotonic solution (75 mM KCl), incubated at 37°C for 7 minutes, and fixed as was previously described (Zhang et al., 2012). After fixation, cells were concentrated and dropped onto an angled, humidified microscope slide, dried, and stained with Hoechst dye (1:1,000) for 60 minutes in the dark. Images were taken at a 100x objective via an Olympus Fluorescence Microscope (Olympus America Inc., Center Valley, Pennsylvania).

RNA Extraction

RNA was extracted from HeLa and HeLa/H1.3(H) using TRIzol Reagent (Invitrogen, Carlsbad, California) according to the manufacturer's protocol. Briefly, cells grown in monolayer were lysed (by adding 0.5 ml of TRIzol reagent) and homogenized. After incubation at room temperature for 5 minutes, 1/5 volume of chloroform was added and the tube were shaken vigorously for 15 seconds and incubated at room temperature for 2-3 minutes. The mixtures were subsequently centrifuged at 12,000 g for 15 minutes at 2-8°C, the RNA-containing colorless aqueous phase was transferred into a fresh tube, and 1/2 volume of isopropanol was added. After incubation at room temperature for 10 minutes, RNA was pelleted by centrifugation at 12,000 g for 10 minutes, and the pellet was washed with 75% ethanol, 95 % ethanol, air dried, and dissolved in RNase-free water. The RNA concentration was measured using Nanodrop 1000 (Thermo Scientific, Wilmington, DE) and gel electrophoresis was performed to determine RNA quality.

Quantitative Reverse Transcription PCR (qRT-PCR)

The synthesis of the first-strand cDNA from 2.5 µg total RNA extracted from HeLa cells was performed using the SuperScript III (SSIII) First-Strand Synthesis System for RT-PCR (Invitrogen, Carlsbad, California) according to the manufacturer's protocol. Briefly, RNase-free water and RNA were added to a 2:1:1 ratio of dNTP to random hexamers (random primers) and oligodT respectively for a total of 1 µl per tube. The mix was incubated for 5 minutes at 65°C, then placed on ice for 1 minute. For the cDNA mix, 5x Buffer was added to 0.1 M DTT, SSIII RT (200 U/µl), and RNaseOUT (40 U/µl). This

cDNA mix was added to each RNA/primer mix. Using a PCR machine, the total reaction mixture (10 µl total per reaction) was carried out at 25°C for 10 minutes, followed by 50 minutes at 50°C, 5 minutes at 85°C, and chilled on ice. The resulting cDNA were immediately used for qRT-PCR or stored at -20°C for future use.

The cDNA was analyzed by quantitative real-time PCR as previously described (Medrzycki, 2013). PCR primers used for quantitative analysis of the different FLAG-H1 subtypes were developed by a PhD graduate from our lab, Dr. Magdalena Medrzycki, and are listed in table 3. iQ SYBR green PCR Supermix kit (BioRad, Hercules, California) in a MyIQ Single Color RT-PCR detection system was used to quantify and analyze the amounts of cDNA from both HeLa and HeLa/H1.3(H). Samples were loaded on a Microseal 96-well PCR plate (BioRad) and analyzed in duplicates. For this experiment, the following program was applied: 3 minutes at 95°C; followed by 40 cycles of 10 seconds at 95°C, 20 seconds at 60°C, 30 seconds at 72°C; and ended with 1 minute at 95°C. Then iQ5 Optical System software version 2.0 supplied by the manufacturer was used to record and quantify the expression levels of the different genes. The expression levels of the FLAG-H1 genes were normalized against those of a house-keeping gene, GAPDH (Glyceraldehyde-3-phosphate dehydrogenase), and graphs of the relative expression were created.

Table 3. Primer list for qRT-PCR analysis of FLAG-H1s and GAPDH

Gene	Sequence
FLAG-H1.0	F: ACAAAGACGATGACGACAAG R: GAAGGCCACTGACTTCTTGG
FLAG-H1.1	F: ACAAAGACGATGACGACAAG R: GGCTGCTGCAGCCTTAGCAGGT
FLAG-H1.2	F: ACAAAGACGATGACGACAAG R: ACGAGGCGTACCCCCAGCCTTT
FLAG-H1.3	F: ACAAAGACGATGACGACAAG R: TTGCGCCTGCCTTCTTCGCCTTT
FLAG-H1.4	F: ACAAAGACGATGACGACAAG R: GCGCTTGGCCGCACCTGCAGAC
FLAG-H1.5	F: ACAAAGACGATGACGACAAG R: AGCAGCGCCGGCGCCGGCAGCC
GAPDH	F: GAGTCAACGGATTTGGTCGT R: GACAAGCTTCCCGTTCTCAG

Statistical Analysis

An unpaired two-tailed student's t-test with 95% confidence intervals was performed and graphs were generated using Microsoft Excel 2010 software (Microsoft Corporation, Redmond, WA). P-values less than 0.05 were considered statistically significant.

CHAPTER 3

RESULTS

3.1 Analysis of the differential expression patterns of individual linker histone H1 variants in HeLa and HeLa/H1.3(H) cells

HeLa is an immortal cancer cell line derived from cervical cancer and is frequently used in cancer research. To quantitatively measure the expression patterns of individual linker histone H1 subtypes in HeLa cells, we performed RP-HPLC of total histones extracted from HeLa cells. The different linker histone variants were separated based on their hydrophobicity on HPLC following an increasing gradient of acetonitrile/0.1% TFA as described in Materials and Methods. HPLC profiles displayed two H1 peaks which were collected, lyophilized, and analyzed by Western blotting and Mass Spectrometry. Such analyses indicated that the first peak contains H1.5 and second peak contains H1.2, H1.3, and H1.4 (Figure 3).

Previous studies from our lab have identified Top2a as a novel H1.3 binding partner and demonstrated that overexpression of H1.3 in HeLa cells leads to an increased cell proportion with chromosome bridges (Lasater, 2012). To quantitatively assess the level of expression of H1 variants in HeLa/H1.3(H) cells (Lasater, 2012), we performed HPLC analysis of total histone extracts from HeLa/H1.3(H) cells. Compared with HeLa cells, HeLa/H1.3(H) cells had an increased proportion of peak 2 and a decrease level of peak 1 in the HPLC profile (Figure 3A). Western blotting assays show that FLAG-hH1.3 was co-eluted with the endogenous H1.3 protein in the peak #2, indicating that exogenous H1.3s have the same biochemical properties as the endogenous. Also, a

stronger band of FLAG-H1.3 than H1.3 in the second fraction was detected in Western blotting with anti-H1.3 antibody, reflecting a significantly higher amount of FLAG-H1.3 compared to the endogenous counterpart (Figure 3B and Figure 4). The presence and significant amount of FLAG-H1.3 in the peak #2 was further confirmed by Mass Spectrometry analysis of proteins present in the peak #2 (Figure 3C). qRT-PCR assays using primers specific to the FLAG-H1 variants as described in Materials and Methods also indicate the overexpression of FLAG-H1.3 and the lack of expression of other FLAG-H1 subtypes (Figure 5).

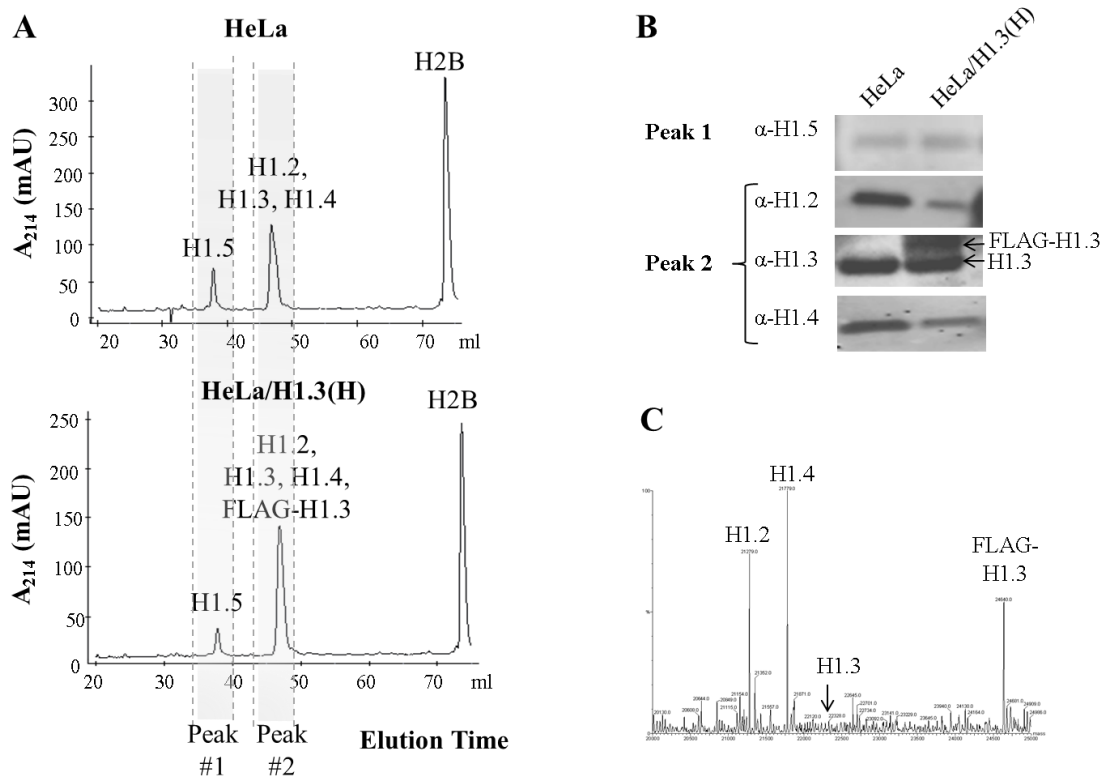


Figure 3. Analysis of total histone extracts from HeLa and HeLa/H1.3(H) cells. (A) RP-HPLC analysis of total extracts from HeLa and HeLa/H1.3(H). **(B)** Western blot of Peak 1 and peak 2 eluted from HPLC. **(C)** Mass spectrometry analysis of peak 2 eluted from HPLC of HeLa/H1.3(H) cells. The H1 variants are labeled above the corresponding peaks.

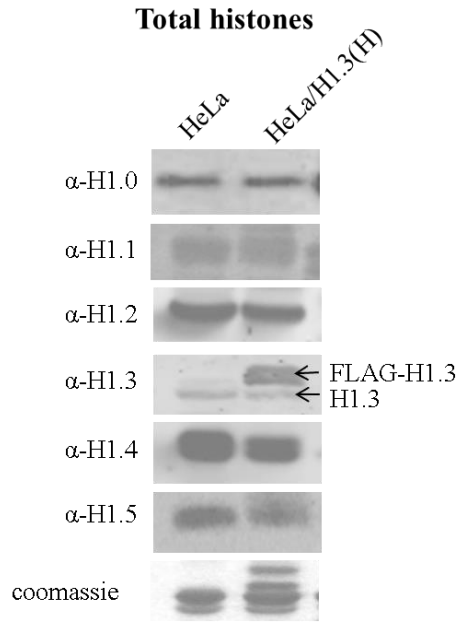


Figure 4. Western blotting analysis of total histone extracts from HeLa and HeLa/H1.3(H) cells. Coomassie stain of total histone extracts (20 μ g) was included as loading control.

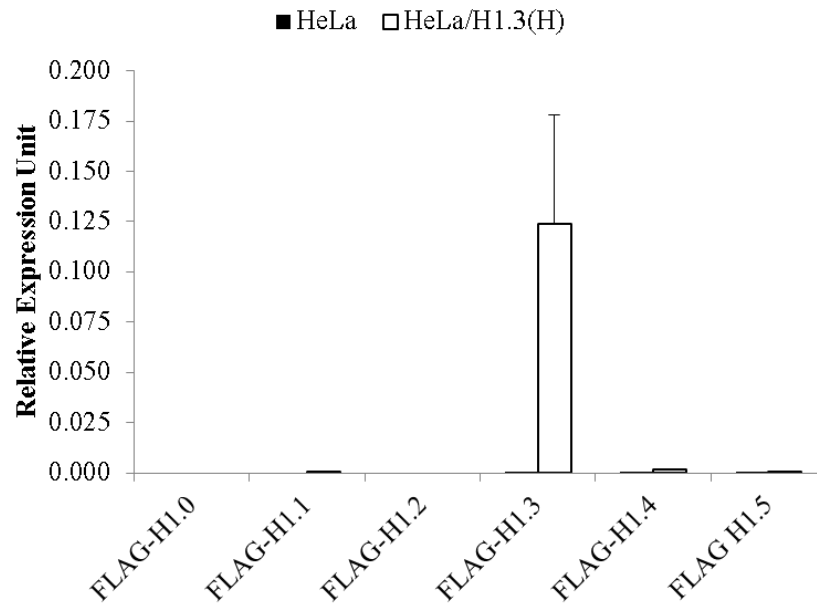


Figure 5. qRT-PCR analysis of mRNA levels of FLAG-tagged linker histone subtypes in HeLa and HeLa/H1.3(H) cells. Gene expression levels of FLAG-H1s were normalized over that of GAPDH.

To quantify and compare the protein levels of individual H1 subtypes and the total H1s in HeLa and HeLa/H1.3(H) cells, we calculated H1 to nucleosome ratio according to the HPLC analysis (representative profiles shown in Figure 3A) as described in Materials and Methods. Such analysis showed that the total H1 to nucleosome ratios were 0.67 and 0.96 in HeLa and HeLa/H1.3(H), respectively. These results indicate that overexpression of FLAGH1.3 leads to a 43% increase of the total H1 levels in HeLa/H1.3(H) compared with HeLa cells (Figure 6A). This increase is due to the overexpression of FLAGH1.3 which also leads to the reduced percentage of H1.5, and a likely decrease in levels of H1.2 and H1.4 among the total H1s (Figure 6B).

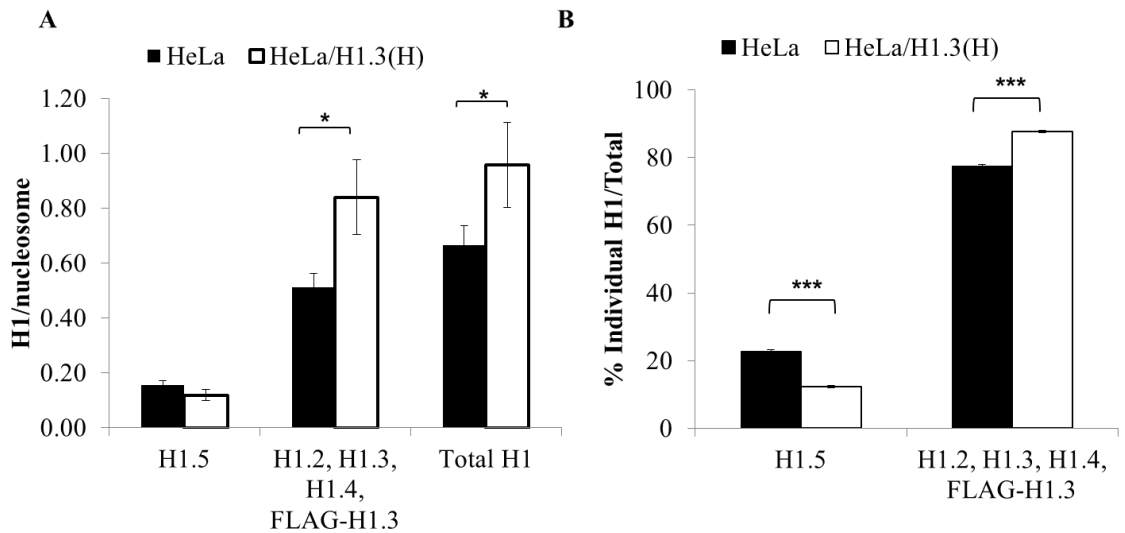


Figure 6. Overexpression of linker histone H1.3 increases total H1 levels and changes H1 composition in HeLa cells. The H1 to nucleosome ratio (A) and the percentage of total histone (B) of HeLa and HeLa/H1.3(H) cells were calculated as described in Materials and Methods. Results were obtained from three independent experiments. * $p < 0.05$; *** $p < 0.0001$.

3.2 Top2 co-localizes with linker histone H1 *in vivo*

Previous co-immunoprecipitation and western-blot data from our lab have shown that histone H1.3, the most abundant H1 variant in mouse ESCs (Fan et al., 2005), interacts with Top2a *in vivo* (Lasater, 2012) and Xu and Fan, unpublished observation). To further investigate the cellular localization of H1 and Top2a, we performed immunostaining of HeLa/H1.3(H) cells using anti-FLAG and anti-Top2a antibodies as described in Materials and Methods. The results indicate a co-localization of H1 and Top2a in the nucleus (Figure 7), further supporting the interaction of H1 and Top2a *in vivo*.

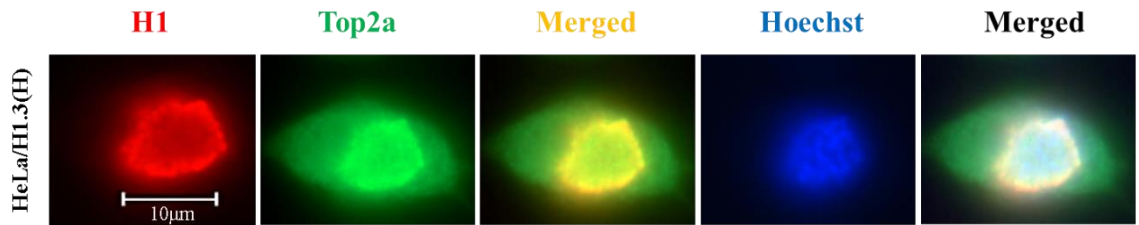


Figure 7. Top2a co-localizes with H1 *in vivo*. Scale bar: 10µm

3.3 Over-expressing hH1.3 in HeLa cells leads to increased cell population with abnormal chromosomes

Top2a is essential for chromatin disentanglement, separation of sister chromatids, and chromosome condensation (Baxter & Aragon, 2012; Gonzalez et al., 2011; Li et al., 2013; Samejima et al., 2012). Since we previously demonstrated that H1 inhibits Top2a activity (Lasater, 2012), we set out to compare the mitotic chromosome morphologies of

HeLa and HeLa/H1.3(H) cells. Cells arrested at metaphase using colcemid and metaphase spreads of each of the cell lines were prepared as described in Materials and Methods. The majority of cells had normal mitotic chromosomes morphology with distinct and condensed chromosomes, while a small fraction of cells displayed abnormal chromosome morphology with long, entangled or uncondensed chromosomes (Figure 8A). We observed a significantly higher percentage of undercondensed and entangled chromosomes from the metaphase spreads of HeLa/H1.3 cells compared to those from HeLa or HeLa/EV control cell lines (Figure 8B). Results from three independent blind-counting experiments (75 metaphase spreads per cell line per experiment) demonstrated that HeLa and HeLa/EV cells (HeLa cells transfected with an empty vector) had respective 12.94% and 9.35% of cells with abnormal chromosomes morphology compared with 28.40% and 21.07% of respective HeLa/H1.3(H) and HeLa/H1.3(M) cells. These results suggest that H1.3 overexpression inhibits chromosome condensation and segregation, mimicking the abnormal mitotic chromosome morphologies observed in cells treated with Top2a siRNA and shRNA (Bower et al., 2010; Lane, Gimenez-Abian, & Clarke, 2013). These results support an inhibitory role of H1 on Top2a, which likely contributes to the effects of over-expression of H1.3 on mitotic chromosome.

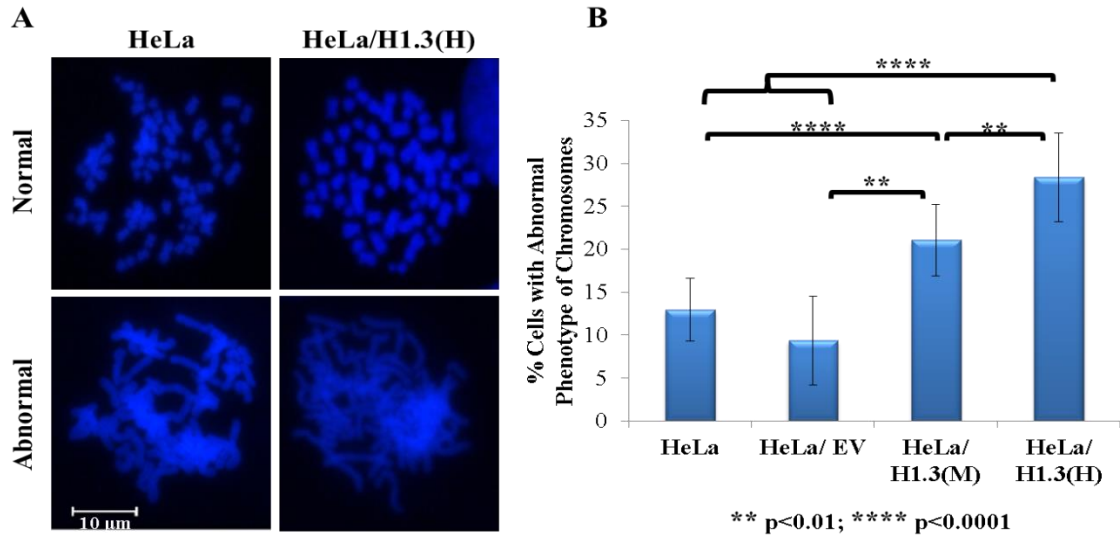


Figure 8. Over-expressing hH1.3 in HeLa cells leads to increased cell population with abnormal chromosomes. (A) Representative metaphase spread images showing normal, entangled and undercondensed chromosomes. Scale bar: 10 μm (B) Percent of cells with abnormal chromosomes of HeLa, HeLa/EV, HeLa/H1.3(M) and HeLa/H1.3(H) cells. P values were calculated using a student's t-test analysis.

3.4 Over-expressing hH1.3 in HeLa cells inhibits cell growth

To further characterize the phenotypic changes resulting from over-expressing hH1.3 in HeLa cells, we analyzed growth rate and metabolic activity by growth curve and MTT assays. The MTT assay measures the ability of the mitochondrial enzyme, succinate dehydrogenase, to cleave the yellow tetrazolium salt to form the purple, water insoluble, formazan crystals. This reduction reaction in the mitochondria of living cells is an indicator of the viability and proliferative activity of the cells (Mosmann, 1983). HeLa/H1.3(H) cells displayed a slower growth rate and a decrease in metabolic activity compared to HeLa cells ($p<0.0001$) (Figure 9). The doubling time during the exponential

growth phase (days 2-6) was calculated based on the cell numbers relative to the initial seeding (day 0). HeLa had a doubling time of 23.60 ± 1.33 hours, similar to the 24 hours reported in the literature (Stephenson, 1982), whereas HeLa/H1.3(H) cells had a doubling time of 27.75 ± 1.68 hours ($p < 0.0001$), a 16.18% increase, suggesting an inhibition on cell growth rate by H1.3 overexpression. HeLa/EV cells (HeLa cells transfected with empty vector) displayed no significant difference in growth curve and MTT assays from HeLa cells (data not shown).

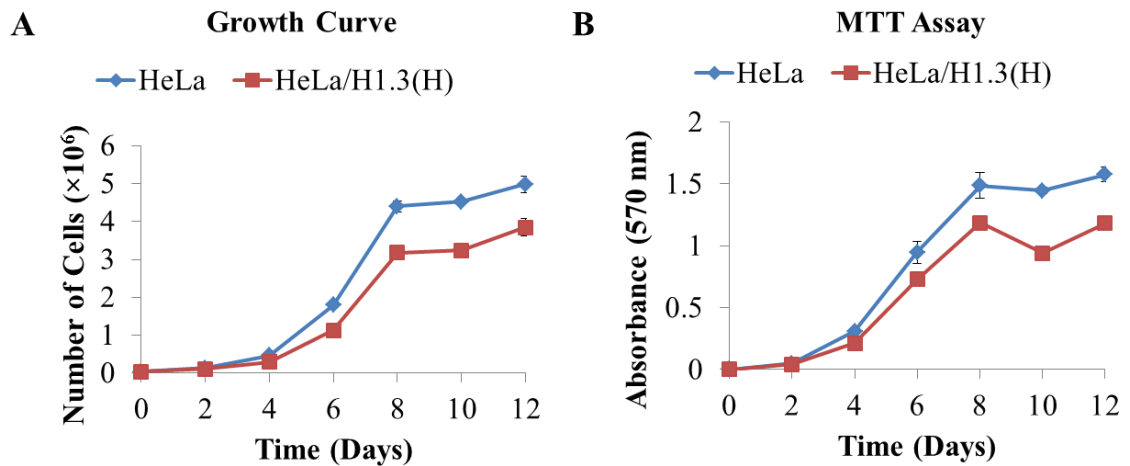


Figure 9. Over-expressing hH1.3 in HeLa cells leads to delayed growth and decreased metabolic activity (A) A graph showing the growth rate and (B) MTT assay for HeLa and HeLa/H1.3(H) ($p < 0.0001$)

3.5 H1 inhibition of Top2a does not proceed via the Top2a-DNA complex

To investigate the mechanism of inhibition of Top2a by H1.3, we examine the production of DNA-Topo complexes using the topoisomerase *in vivo* link assay as described in Materials and Methods. This assay resolves DNA-Top2 complexes on a CsCl gradient. Different fractions collected from ultracentrifugation were measured for DNA content at OD₂₆₀ and for Top2 levels using a dot blot and immunoblotting. HeLa and HeLa/H1.3(H) cells were treated with etoposide, a topoisomerase inhibitor that stabilizes DNA-Top2 cleavage complexes and causes double-strand breaks (Pommier et al., 2010). As expected, treatment with etoposide resulted in decreased cell numbers (Figure 10A). HeLa cells treated with etoposide had a significant peak at fraction 11 where high DNA content coincides with a strong Top2 signal, indicating the DNA-Top2 complex (Figure 10B&C). However, HeLa, HeLa/H1.3(H), and HeLa/H1.3(H)/etoposide cells did not show significant amount of DNA-Topo complex (Figure 10B&C). This suggests that H1 inhibition of Top2a is probably not through the DNA-Topo complex. In addition, HeLa/H1.3(H) cells treated with etoposide had a significant lower Top2-DNA complex peak than that of HeLa treated with etoposide, suggesting a possible competitive inhibitory effect of H1 with etoposide on Top2a. Alternatively, this may suggest that the inhibition of Top2a by H1 occurs before Top2a forms a complex with DNA.

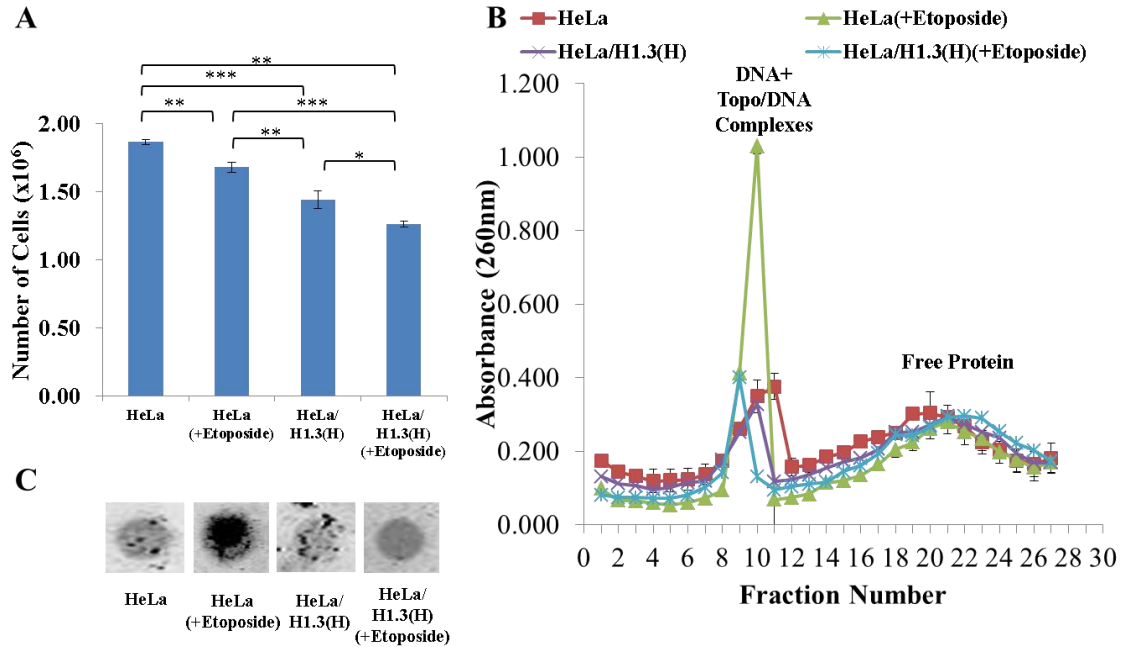


Figure 10. H1 inhibition of Top2a does not proceed via the Top2-DNA complex. (A) The number of HeLa and HeLa/H1.3(H) cells with and without treatment of 100uM of the topoisomerase II inhibitory drug etoposide (* p<0.05; ** p<0.01; *** p<0.001). (B) Absorbance at 260 nm of 27 collected fractions after ultracentrifugation with the Topo-DNA and free protein peaks identified. (C) Representative images of Western blots of fractions with strongest signals using anti-Top2a antibody.

CHAPTER 4

DISCUSSION AND CONCLUSION

In this study, we have further investigated the inhibition of topoisomerase II alpha by linker histone H1. Previous studies from our lab have demonstrated the interaction with and inhibition of Top2a by H1 *in vitro* and also suggested a role of H1 in inhibiting Top2a activity *in vivo*. In this thesis, characterization of HeLa cells overexpressing hH1.3 provides additional evidence supporting an interaction with and inhibition of Top2a by linker histone H1. Furthermore, we found that overexpression of hH1.3 significantly suppressed the growth and metabolism of HeLa cancer cells and resulted in an increased cell population with abnormal mitotic chromosomes. Combining these results with our previous studies, we propose a working model in which inhibition of Top2a activity by H1 results in defects in chromosome condensation and segregation (Figure 11).

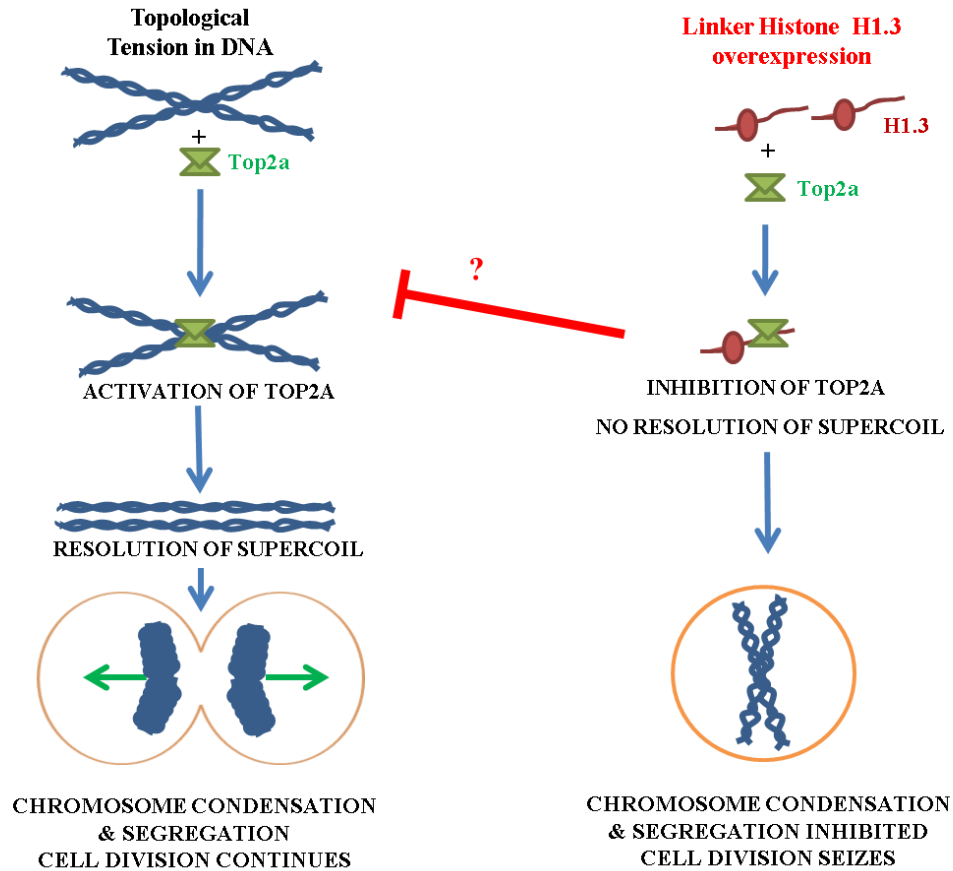


Figure 11. Working Model of the interaction of H1 and Top2a and the effect of the inhibition on chromosome condensation and segregation

When it comes to chromatin structure and function, numerous studies illustrated that Top2a plays a key role in chromosome compaction and the maintenance of a condensed conformation during mitosis (Chang, Goulding, Earnshaw, & Carmena, 2003; Downes et al., 1994; Maeshima & Laemmli, 2003). Similarly, linker histone H1 is a major contributor for chromosome compaction. When H1 was depleted in *Xenopus laevis* egg extracts, and when Top2a was inhibited in *Indian Muntjac* mammalian cells, chromosomes were prevented from properly aligning at the metaphase plate (Downes et al., 1994; Maresca, Freedman, & Heald, 2005). This inhibition of Top2a resulted in a

considerably thinner and longer chromosome morphology (Downes et al., 1994; Maresca et al., 2005). Here, we found a statistically significant increase of the undercondensed and entangled chromosomes when hH1.3 was overexpressed in HeLa cells (Figure 8). This may be due to the inhibitory effects of hH1.3 on Top2a activity. Future studies of Top2a knockdown experiment on hH1.3 cells would help determine if the increase in the abnormal chromosomes is due to the inhibitory effects of hH1.3 on Top2a or caused by other functions of H1.3.

As a follow up on the possible mechanism of the inhibition, we found that H1 does not inhibit Top2a via a DNA-Topo complex measured by the topoisomerase II *in vivo* link assay. Etoposide, a commonly used inhibitor of eukaryotic Topo II, covalently attaches to DNA and prevents the religation by Topo II, thereby resulting in DNA double-strand breaks (Baldwin & Osheroff, 2005; Favoni & Florio, 2011; Ross, Rowe, Glisson, Yalowich, & Liu, 1984). In the topoisomerase II *in vivo* link assay, etoposide treatment leads to significant enrichment of DNA-Top2 complex in HeLa cells but not in HeLa/H1.3(H) cells, suggesting that H1.3 may interact with and inhibits Top2a prior to Top2a binding to the DNA to resolve the supercoils during DNA replication. This possibility could be tested using chromatin immunoprecipitation to determine the genomic localization of H1.3 and Top2 in these cells.

In this study, we demonstrate that overexpression of H1.3 inhibits HeLa cell growth. To further ascertain the inhibitory effects of H1.3 on HeLa cells is due to H1.3 overexpression, knockdown of H1.3 in HeLa/H1.3(H) cells could be performed to determine the rescue of the cell growth phenotypes. In addition, further study of the cell

cycle profiles of HeLa/H1.3(H) and HeLa cells could refine our understanding of the mechanism of inhibition on cell growth by H1.3.

Inhibition of Top2a by synthetic molecule induces cell cycle arrest in different human cancer cells (Belluti et al., 2013; Cheng et al., 2012; S. O. Kim et al., 2013; Olszewska, Szymanski, Mikiciuk-Olasik, & Szymanski, 2014). The inhibition of Top2a enzymatic activity can also trigger G2 checkpoint and deletion of Top2a leading to apoptosis (Akimitsu, Adachi, et al., 2003; Akimitsu, Kamura, et al., 2003; Luo et al., 2009; McPherson & Goldenberg, 1998; St Pierre, Wright, Rowe, & Wright, 2002). Although a number of topoisomerase II inhibitors, such as etoposide, have been developed for cancer treatment, they often cause DNA damages to cancer cells and normal neighboring cells as well. The DNA-damaging effect often leads to secondary neoplasms in patients. Therefore, new Top2a inhibitors with higher efficiency, specificity, and selectivity are desired. Our finding on the inhibition of Top2a by H1 could lead to developing new Top2a inhibitors, such as peptide inhibitors for Top2a based on H1. It is highly possible that specific regions of H1, such as a specific H1 domains or subdomains, may be sufficient for Top2a inhibition. In addition, testing on other cancer cell lines is warranted to determine the scope of the inhibitory effects on Top2a by linker histone H1.

REFERENCES

- Akimitsu, N., Adachi, N., Hirai, H., Hossain, M. S., Hamamoto, H., Kobayashi, M., . . . Sekimizu, K. (2003). Enforced cytokinesis without complete nuclear division in embryonic cells depleting the activity of DNA topoisomerase IIalpha. *Genes Cells*, 8(4), 393-402.
- Akimitsu, N., Kamura, K., Tone, S., Sakaguchi, A., Kikuchi, A., Hamamoto, H., & Sekimizu, K. (2003). Induction of apoptosis by depletion of DNA topoisomerase IIalpha in mammalian cells. *Biochem Biophys Res Commun*, 307(2), 301-307.
- Al-Kuraya, K., Novotny, H., Bavi, P., Siraj, A. K., Uddin, S., Ezzat, A., . . . Tornillo, L. (2007). HER2, TOP2A, CCND1, EGFR and C-MYC oncogene amplification in colorectal cancer. *J Clin Pathol*, 60(7), 768-772. doi: 10.1136/jcp.2006.038281
- Albig, W., Kardalidou, E., Drabent, B., Zimmer, A., & Doenecke, D. (1991). Isolation and characterization of two human H1 histone genes within clusters of core histone genes. *Genomics*, 10(4), 940-948.
- Albig, W., Meergans, T., & Doenecke, D. (1997). Characterization of the H1.5 gene completes the set of human H1 subtype genes. *Gene*, 184(2), 141-148.
- Baldwin, E. L., & Osheroff, N. (2005). Etoposide, topoisomerase II and cancer. *Curr Med Chem Anticancer Agents*, 5(4), 363-372.
- Baxter, J., & Aragon, L. (2012). A model for chromosome condensation based on the interplay between condensin and topoisomerase II. *Trends Genet*, 28(3), 110-117. doi: 10.1016/j.tig.2011.11.004
- Bednar, J., Horowitz, R. A., Grigoryev, S. A., Carruthers, L. M., Hansen, J. C., Koster, A. J., & Woodcock, C. L. (1998). Nucleosomes, linker DNA, and linker histone form a unique structural motif that directs the higher-order folding and compaction of chromatin. *Proc Natl Acad Sci U S A*, 95(24), 14173-14178.
- Belluti, S., Basile, V., Benatti, P., Ferrari, E., Marverti, G., & Imbriano, C. (2013). Concurrent inhibition of enzymatic activity and NF-Y-mediated transcription of Topoisomerase-IIalpha by bis-DemethoxyCurcumin in cancer cells. *Cell Death Dis*, 4, e756. doi: 10.1038/cddis.2013.287

- Bower, J. J., Karaca, G. F., Zhou, Y., Simpson, D. A., Cordeiro-Stone, M., & Kaufmann, W. K. (2010). Topoisomerase II α maintains genomic stability through decatenation G(2) checkpoint signaling. *Oncogene*, 29(34), 4787-4799. doi: 10.1038/onc.2010.232
- Brown, D. T. (2001). Histone variants: are they functionally heterogeneous? *Genome Biol*, 2(7), Reviews0006.
- Brown, D. T. (2003). Histone H1 and the dynamic regulation of chromatin function. *Biochem Cell Biol*, 81(3), 221-227. doi: 10.1139/o03-049
- Brown, D. T., Alexander, B. T., & Sittman, D. B. (1996). Differential effect of H1 variant overexpression on cell cycle progression and gene expression. *Nucleic Acids Res*, 24(3), 486-493.
- Caterino, T. L., Fang, H., & Hayes, J. J. (2011). Nucleosome linker DNA contacts and induces specific folding of the intrinsically disordered H1 carboxyl-terminal domain. *Mol Cell Biol*, 31(11), 2341-2348. doi: 10.1128/mcb.05145-11
- Chang, C. J., Goulding, S., Earnshaw, W. C., & Carmena, M. (2003). RNAi analysis reveals an unexpected role for topoisomerase II in chromosome arm congression to a metaphase plate. *J Cell Sci*, 116(Pt 23), 4715-4726. doi: 10.1242/jcs.00797
- Cheng, M. H., Yang, Y. C., Wong, Y. H., Chen, T. R., Lee, C. Y., Yang, C. C., . . . Chiu, H. F. (2012). B1, a novel topoisomerase II inhibitor, induces apoptosis and cell cycle G1 arrest in lung adenocarcinoma A549 cells. *Anticancer Drugs*, 23(2), 191-199. doi: 10.1097/CAD.0b013e32834cd277
- Daujat, S., Zeissler, U., Waldmann, T., Happel, N., & Schneider, R. (2005). HP1 binds specifically to Lys26-methylated histone H1.4, whereas simultaneous Ser27 phosphorylation blocks HP1 binding. *J Biol Chem*, 280(45), 38090-38095. doi: 10.1074/jbc.C500229200
- Downes, C. S., Clarke, D. J., Mullinger, A. M., Gimenez-Abian, J. F., Creighton, A. M., & Johnson, R. T. (1994). A topoisomerase II-dependent G2 cycle checkpoint in mammalian cells. *Nature*, 372(6505), 467-470. doi: 10.1038/372467a0
- Earnshaw, W. C., Halligan, B., Cooke, C. A., Heck, M. M., & Liu, L. F. (1985). Topoisomerase II is a structural component of mitotic chromosome scaffolds. *J Cell Biol*, 100(5), 1706-1715.

- Espeli, O., & Mariani, K. J. (2004). Untangling intracellular DNA topology. *Mol Microbiol*, 52(4), 925-931. doi: 10.1111/j.1365-2958.2004.04047.x
- Fan, Y., Nikitina, T., Morin-Kensicki, E. M., Zhao, J., Magnuson, T. R., Woodcock, C. L., & Skoultchi, A. I. (2003). H1 linker histones are essential for mouse development and affect nucleosome spacing in vivo. *Mol Cell Biol*, 23(13), 4559-4572.
- Fan, Y., Nikitina, T., Zhao, J., Fleury, T. J., Bhattacharyya, R., Bouhassira, E. E., . . . Skoultchi, A. I. (2005). Histone H1 depletion in mammals alters global chromatin structure but causes specific changes in gene regulation. *Cell*, 123(7), 1199-1212. doi: 10.1016/j.cell.2005.10.028
- Fan, Y., Sirotkin, A., Russell, R. G., Ayala, J., & Skoultchi, A. I. (2001). Individual somatic H1 subtypes are dispensable for mouse development even in mice lacking the H1(0) replacement subtype. *Mol Cell Biol*, 21(23), 7933-7943. doi: 10.1128/mcb.21.23.7933-7943.2001
- Fan, Y., & Skoultchi, A. I. (2004). Genetic analysis of H1 linker histone subtypes and their functions in mice. *Methods Enzymol*, 377, 85-107. doi: 10.1016/s0076-6879(03)77005-0
- Favoni, R. E., & Florio, T. (2011). Combined chemotherapy with cytotoxic and targeted compounds for the management of human malignant pleural mesothelioma. *Trends Pharmacol Sci*, 32(8), 463-479. doi: 10.1016/j.tips.2011.03.011
- Garrett, M. D., & Collins, I. (2011). Anticancer therapy with checkpoint inhibitors: what, where and when? *Trends Pharmacol Sci*, 32(5), 308-316. doi: 10.1016/j.tips.2011.02.014
- Gonzalez, R. E., Lim, C. U., Cole, K., Bianchini, C. H., Schools, G. P., Davis, B. E., . . . Broude, E. V. (2011). Effects of conditional depletion of topoisomerase II on cell cycle progression in mammalian cells. *Cell Cycle*, 10(20), 3505-3514. doi: 10.4161/cc.10.20.17778
- Hansen, J. C., Lu, X., Ross, E. D., & Woody, R. W. (2006). Intrinsic protein disorder, amino acid composition, and histone terminal domains. *J Biol Chem*, 281(4), 1853-1856. doi: 10.1074/jbc.R500022200

- Happel, N., & Doenecke, D. (2009). Histone H1 and its isoforms: contribution to chromatin structure and function. *Gene*, 431(1-2), 1-12. doi: 10.1016/j.gene.2008.11.003
- Harshman, S. W., Young, N. L., Parthun, M. R., & Freitas, M. A. (2013). H1 histones: current perspectives and challenges. *Nucleic Acids Res*, 41(21), 9593-9609. doi: 10.1093/nar/gkt700
- Heck, M. M., Hittelman, W. N., & Earnshaw, W. C. (1988). Differential expression of DNA topoisomerases I and II during the eukaryotic cell cycle. *Proc Natl Acad Sci U S A*, 85(4), 1086-1090.
- Horn, P. J., & Peterson, C. L. (2002). Molecular biology. Chromatin higher order folding-wrapping up transcription. *Science*, 297(5588), 1824-1827. doi: 10.1126/science.1074200
- Jedrusik, M. A., & Schulze, E. (2001). A single histone H1 isoform (H1.1) is essential for chromatin silencing and germline development in *Caenorhabditis elegans*. *Development*, 128(7), 1069-1080.
- Kalashnikova, A. A., Winkler, D. D., McBryant, S. J., Henderson, R. K., Herman, J. A., DeLuca, J. G., . . . Hansen, J. C. (2013). Linker histone H1.0 interacts with an extensive network of proteins found in the nucleolus. *Nucleic Acids Res*, 41(7), 4026-4035. doi: 10.1093/nar/gkt104
- Kim, K., Jeong, K. W., Kim, H., Choi, J., Lu, W., Stallcup, M. R., & An, W. (2012). Functional interplay between p53 acetylation and H1.2 phosphorylation in p53-regulated transcription. *Oncogene*, 31(39), 4290-4301. doi: 10.1038/onc.2011.605
- Kim, S. O., Sakchaisri, K., Thimmegowda, N. R., Soung, N. K., Jang, J. H., Kim, Y. S., . . . Kim, B. Y. (2013). STK295900, a dual inhibitor of topoisomerase 1 and 2, induces G(2) arrest in the absence of DNA damage. *PLoS One*, 8(1), e53908. doi: 10.1371/journal.pone.0053908
- Lane, A. B., Gimenez-Abian, J. F., & Clarke, D. J. (2013). A novel chromatin tether domain controls topoisomerase IIalpha dynamics and mitotic chromosome formation. *J Cell Biol*, 203(3), 471-486. doi: 10.1083/jcb.201303045
- Larsen, A. K., Skladanowski, A., & Bojanowski, K. (1996). The roles of DNA topoisomerase II during the cell cycle. *Prog Cell Cycle Res*, 2, 229-239.

- Lasater, S. (2012). *An investigation of the interaction of linker histone H1 with topoisomerase II alpha*. (Unpublished Master's Thesis), Georgia Institute of Technology, Atlanta, GA.
- Li, X. M., Yu, C., Wang, Z. W., Zhang, Y. L., Liu, X. M., Zhou, D., . . . Fan, H. Y. (2013). DNA topoisomerase II is dispensable for oocyte meiotic resumption but is essential for meiotic chromosome condensation and separation in mice. *Biol Reprod*, 89(5), 118. doi: 10.1095/biolreprod.113.110692
- Liu, X., Zou, H., Widlak, P., Garrard, W., & Wang, X. (1999). Activation of the apoptotic endonuclease DFF40 (caspase-activated DNase or nuclease). Oligomerization and direct interaction with histone H1. *J Biol Chem*, 274(20), 13836-13840.
- Lu, X., Hamkalo, B., Parseghian, M. H., & Hansen, J. C. (2009). Chromatin condensing functions of the linker histone C-terminal domain are mediated by specific amino acid composition and intrinsic protein disorder. *Biochemistry*, 48(1), 164-172. doi: 10.1021/bi801636y
- Luger, K., Mader, A. W., Richmond, R. K., Sargent, D. F., & Richmond, T. J. (1997). Crystal structure of the nucleosome core particle at 2.8 Å resolution. *Nature*, 389(6648), 251-260. doi: 10.1038/38444
- Luo, K., Yuan, J., Chen, J., & Lou, Z. (2009). Topoisomerase IIalpha controls the decatenation checkpoint. *Nat Cell Biol*, 11(2), 204-210. doi: 10.1038/ncb1828
- Maeshima, K., & Laemmli, U. K. (2003). A two-step scaffolding model for mitotic chromosome assembly. *Dev Cell*, 4(4), 467-480.
- Maresca, T. J., Freedman, B. S., & Heald, R. (2005). Histone H1 is essential for mitotic chromosome architecture and segregation in *Xenopus laevis* egg extracts. *J Cell Biol*, 169(6), 859-869. doi: 10.1083/jcb.200503031
- McBryant, S. J., Lu, X., & Hansen, J. C. (2010). Multifunctionality of the linker histones: an emerging role for protein-protein interactions. *Cell Res*, 20(5), 519-528. doi: 10.1038/cr.2010.35
- McClendon, A. K., & Osheroff, N. (2007). DNA topoisomerase II, genotoxicity, and cancer. *Mutat Res*, 623(1-2), 83-97. doi: 10.1016/j.mrfmmm.2007.06.009

- McClendon, A. K., Rodriguez, A. C., & Osheroff, N. (2005). Human topoisomerase IIalpha rapidly relaxes positively supercoiled DNA: implications for enzyme action ahead of replication forks. *J Biol Chem*, 280(47), 39337-39345. doi: 10.1074/jbc.M503320200
- McPherson, J. P., & Goldenberg, G. J. (1998). Induction of apoptosis by deregulated expression of DNA topoisomerase IIalpha. *Cancer Res*, 58(20), 4519-4524.
- Medrzycki, M. (2013). *The role of H1 linker histone variants in ovarian cancer*. (Unpublished Doctoral Dissertation), Georgia Institute of Technology, Atlanta, GA.
- Medrzycki, M., Zhang, Y., Cao, K., & Fan, Y. (2012). Expression analysis of mammalian linker-histone subtypes. *J Vis Exp*(61). doi: 10.3791/3577
- Meergans, T., Albig, W., & Doenecke, D. (1997). Varied expression patterns of human H1 histone genes in different cell lines. *DNA Cell Biol*, 16(9), 1041-1049.
- Millan-Arino, L., Islam, A. B., Izquierdo-Bouldstridge, A., Mayor, R., Terme, J. M., Luque, N., . . . Jordan, A. (2014). Mapping of six somatic linker histone H1 variants in human breast cancer cells uncovers specific features of H1.2. *Nucleic Acids Res*, 42(7), 4474-4493. doi: 10.1093/nar/gku079
- Misteli, T., Gunjan, A., Hock, R., Bustin, M., & Brown, D. T. (2000). Dynamic binding of histone H1 to chromatin in living cells. *Nature*, 408(6814), 877-881. doi: 10.1038/35048610
- Mondal, N., & Parvin, J. D. (2001). DNA topoisomerase IIalpha is required for RNA polymerase II transcription on chromatin templates. *Nature*, 413(6854), 435-438. doi: 10.1038/35096590
- Mondal, N., Zhang, Y., Jonsson, Z., Dhar, S. K., Kannapiran, M., & Parvin, J. D. (2003). Elongation by RNA polymerase II on chromatin templates requires topoisomerase activity. *Nucleic Acids Res*, 31(17), 5016-5024.
- Montes de Oca, R., Lee, K. K., & Wilson, K. L. (2005). Binding of barrier to autointegration factor (BAF) to histone H3 and selected linker histones including H1.1. *J Biol Chem*, 280(51), 42252-42262. doi: 10.1074/jbc.M509917200

- Mosmann, T. (1983). Rapid colorimetric assay for cellular growth and survival: application to proliferation and cytotoxicity assays. *J Immunol Methods*, 65(1-2), 55-63.
- Oberg, C., Izzo, A., Schneider, R., Wrangé, O., & Belikov, S. (2012). Linker histone subtypes differ in their effect on nucleosomal spacing in vivo. *J Mol Biol*, 419(3-4), 183-197. doi: 10.1016/j.jmb.2012.03.007
- Olszewska, P., Szymanski, J., Mikiciuk-Olasik, E., & Szymanski, P. (2014). New cyclopentaquinoline derivatives with fluorobenzoic acid induce G1 arrest and apoptosis in human lung adenocarcinoma cells. *Eur J Pharmacol*, 729, 30-36. doi: 10.1016/j.ejphar.2014.02.003
- Pommier, Y., Leo, E., Zhang, H., & Marchand, C. (2010). DNA topoisomerases and their poisoning by anticancer and antibacterial drugs. *Chem Biol*, 17(5), 421-433. doi: 10.1016/j.chembiol.2010.04.012
- Ramakrishnan, V., Finch, J. T., Graziano, V., Lee, P. L., & Sweet, R. M. (1993). Crystal structure of globular domain of histone H5 and its implications for nucleosome binding. *Nature*, 362(6417), 219-223. doi: 10.1038/362219a0
- Robinson, P. J., & Rhodes, D. (2006). Structure of the '30 nm' chromatin fibre: a key role for the linker histone. *Curr Opin Struct Biol*, 16(3), 336-343. doi: 10.1016/j.sbi.2006.05.007
- Ross, W., Rowe, T., Glisson, B., Yalowich, J., & Liu, L. (1984). Role of topoisomerase II in mediating epipodophyllotoxin-induced DNA cleavage. *Cancer Res*, 44(12 Pt 1), 5857-5860.
- Samejima, K., Samejima, I., Vagnarelli, P., Ogawa, H., Vargiu, G., Kelly, D. A., . . . Earnshaw, W. C. (2012). Mitotic chromosomes are compacted laterally by KIF4 and condensin and axially by topoisomerase IIalpha. *J Cell Biol*, 199(5), 755-770. doi: 10.1083/jcb.201202155
- Sancho, M., Diani, E., Beato, M., & Jordan, A. (2008). Depletion of human histone H1 variants uncovers specific roles in gene expression and cell growth. *PLoS Genet*, 4(10), e1000227. doi: 10.1371/journal.pgen.1000227
- Schrader, C., Meusers, P., Brittinger, G., Teymoortash, A., Siebmann, J. U., Janssen, D., . . . Tiemann, M. (2004). Topoisomerase IIalpha expression in mantle cell

lymphoma: a marker of cell proliferation and a prognostic factor for clinical outcome. *Leukemia*, 18(7), 1200-1206. doi: 10.1038/sj.leu.2403387

Sirotkin, A. M., Edelmann, W., Cheng, G., Klein-Szanto, A., Kucherlapati, R., & Skoultchi, A. I. (1995). Mice develop normally without the H1(0) linker histone. *Proc Natl Acad Sci U S A*, 92(14), 6434-6438.

St Pierre, J., Wright, D. J., Rowe, T. C., & Wright, S. J. (2002). DNA topoisomerase II is essential for preimplantation mouse development. *Mol Reprod Dev*, 61(3), 347-357. doi: 10.1002/mrd.10015

Stephenson, E. M. (1982). Locomotory invasion of human cervical epithelium and avian fibroblasts by HeLa cells in vitro. *J Cell Sci*, 57, 293-314.

Sumner, A. T. (2003). *Chromosomes: Organization and Function*. Oxford: Blackwell Publishers.

Th'ng, J. P., Sung, R., Ye, M., & Hendzel, M. J. (2005). H1 family histones in the nucleus. Control of binding and localization by the C-terminal domain. *J Biol Chem*, 280(30), 27809-27814. doi: 10.1074/jbc.M501627200

Thomas, J. O. (1999). Histone H1: location and role. *Curr Opin Cell Biol*, 11(3), 312-317. doi: 10.1016/s0955-0674(99)80042-8

Wang, J. C. (2002). Cellular roles of DNA topoisomerases: a molecular perspective. *Nat Rev Mol Cell Biol*, 3(6), 430-440. doi: 10.1038/nrm831

Widlak, P., Kalinowska, M., Parseghian, M. H., Lu, X., Hansen, J. C., & Garrard, W. T. (2005). The histone H1 C-terminal domain binds to the apoptotic nuclease, DNA fragmentation factor (DFF40/CAD) and stimulates DNA cleavage. *Biochemistry*, 44(21), 7871-7878. doi: 10.1021/bi050100n

Willman, J. H., & Holden, J. A. (2000). Immunohistochemical staining for DNA topoisomerase II-alpha in benign, premalignant, and malignant lesions of the prostate. *Prostate*, 42(4), 280-286.

Woessner, R. D., Mattern, M. R., Mirabelli, C. K., Johnson, R. K., & Drake, F. H. (1991). Proliferation- and cell cycle-dependent differences in expression of the 170

kilodalton and 180 kilodalton forms of topoisomerase II in NIH-3T3 cells. *Cell Growth Differ*, 2(4), 209-214.

Wolffe, A. P., Khochbin, S., & Dimitrov, S. (1997). What do linker histones do in chromatin? *Bioessays*, 19(3), 249-255. doi: 10.1002/bies.950190311

Wong, W. R., Oliver, A. G., & Linington, R. G. (2012). Development of antibiotic activity profile screening for the classification and discovery of natural product antibiotics. *Chem Biol*, 19(11), 1483-1495. doi: 10.1016/j.chembiol.2012.09.014

Woodcock, C. L., Skoultchi, A. I., & Fan, Y. (2006). Role of linker histone in chromatin structure and function: H1 stoichiometry and nucleosome repeat length. *Chromosome Res*, 14(1), 17-25. doi: 10.1007/s10577-005-1024-3

Zhang, Y., Cooke, M., Panjwani, S., Cao, K., Krauth, B., Ho, P. Y., . . . Fan, Y. (2012). Histone h1 depletion impairs embryonic stem cell differentiation. *PLoS Genet*, 8(5), e1002691. doi: 10.1371/journal.pgen.1002691

Zhao, H., Yu, H., Liu, Y., Wang, Y., & Cai, W. (2008). DNA topoisomerase II-alpha as a proliferation marker in human gliomas: correlation with PCNA expression and patient survival. *Clin Neuropathol*, 27(2), 83-90.

Zlatanova, J., Bishop, T. C., Victor, J. M., Jackson, V., & van Holde, K. (2009). The nucleosome family: dynamic and growing. *Structure*, 17(2), 160-171. doi: 10.1016/j.str.2008.12.016